HHS Public Access

Author manuscript

Mol Cancer Res. Author manuscript; available in PMC 2020 August 01.

Mitotic DNA synthesis is differentially regulated between cancer and non-cancerous cells

Cari L. Graber-Feesl[¶], **Kayla D. Pederson**[¶], **Katherine J. Aney**, **Naoko Shima**[*]

Department of Genetics, Cell Biology and Development, University of Minnesota, at Twin Cities, Masonic Cancer Center, Minneapolis, MN USA

Abstract

Mitotic DNA synthesis is a recently discovered mechanism that resolves late replication intermediates, thereby supporting cell proliferation under replication stress. This unusual form of DNA synthesis occurs in the absence of RAD51 or BRCA2, which led to the identification of RAD52 as a key player in this process. Notably, mitotic DNA synthesis is predominantly observed at chromosome loci that co-localize with FANCD2 foci. However, the role of this protein in mitotic DNA synthesis remains largely unknown. In this study, we investigated the role of FANCD2 and its interplay with RAD52 in mitotic DNA synthesis using aphidicolin as a universal inducer of this process. After examining eight human cell lines, we provide evidence for FANCD2 rather than RAD52 as a fundamental supporter of mitotic DNA synthesis. In *cancer* cell lines, FANCD2 exerts this role independently of RAD52. Surprisingly, RAD52 is dispensable for mitotic DNA synthesis in *non-cancerous* cell lines, but these cells strongly depend on FANCD2 for this process. Therefore, RAD52 functions selectively in cancer cells as a secondary regulator in addition to FANCD2 to facilitate mitotic DNA synthesis. As an alternative to aphidicolin, we found partial inhibition of origin licensing as an effective way to induce mitotic DNA synthesis preferentially in cancer cells. Importantly, cancer cells still perform mitotic DNA synthesis by dual regulation of FANCD2 and RAD52 under such conditions.

Implications—These key differences in mitotic DNA synthesis between cancer and non-cancerous cells advance our understanding of this mechanism and can be exploited for cancer therapies.

Introduction

It is widely accepted that cancer development is closely associated with replication stress (1,2). Studies have demonstrated that over-expression of certain oncogenes in cultured human cells induces replication stress by disturbing the normal kinetics of DNA replication, altering the usage of replication origins and fork speed (3,4). Under such conditions, replication forks are more frequently stalled/collapsed relative to normal S phase, inducing DNA damage (5,6). Consistent with these findings, human precancerous lesions in a wide range of tissues display markers of DNA damage and activated checkpoints (5–8). While

[*]Corresponding author: Naoko Shima, Mailing address: 6-160 Jackson Hall, 321 Church St SE, Minneapolis, MN 55455 USA, Phone: 612-626-7830, FAX; 612-626-6140, shima023@umn.edu.

[¶]Equal contribution

The authors declare no potential conflicts of interest.

such responses act as an anti-tumorigenic barrier by triggering apoptosis or senescence of precancerous cells, a small fraction of cells eventually escapes the barrier to progress cancer development (7,9). It is also possible that precancerous cells develop mechanism(s) that counteract intrinsic replication stress to sustain their survival and proliferation.

Mitotic DNA synthesis (or abbreviated as MiDAS) may be one such mechanism, as it is strongly activated under replication stress (10,11). This unusual timing of DNA synthesis is universally observed in a variety of mammalian cells after treatment with a low dose of Aphidicolin (Aph), a replication inhibitor (10–14). After pulse labeling with EdU (5-ethynyl-2'-deoxyuridine), punctuated sites of mitotic DNA synthesis are described as EdU spots or foci in prophase/prometaphase nuclei (10–14). Even in the absence of Aph, EdU spots can still be observed when the process known as origin licensing is partially inhibited (12,15). Origin licensing strictly occurs from late M to early G1 phase of the cell cycle and is a prerequisite for DNA replication in S phase (16,17). During this process, origin recognition complex (ORC), which is comprised of six subunits, first binds DNA, and with additional proteins helps load hetero-hexamers of mini-chromosome maintenance (MCM) proteins onto ORC-bound DNA (18–22). In the following S phase, a small fraction of licensed origins fire only once when a pair of DNA-bound MCM complexes assemble into active helicases with co-factors to generate bi-directional replication forks (23–25). The rest of licensed origins are known as dormant origins and remain unused or occasionally fire to rescue stalled replication forks (26,27). It is known that the expression of ORC and MCM proteins are generally upregulated in cancer cells (28–30), which may help generate many more dormant origins to counteract intrinsic replication stress they may have. These findings prompted us to test if partial inhibition of origin licensing is an effective way to induce mitotic DNA synthesis in cancer cells.

Mitotic DNA synthesis operates in prophase/prometaphase for the resolution of late replication intermediates to allow disjunction of sister chromatids in anaphase (10,11). However, the underlying mechanism is largely unknown. The current model describes that mitotic DNA synthesis begins processing stalled replication forks with structure-specific endonucleases including MUS81 followed by DNA synthesis which requires POLD3, a non-catalytic subunit of Polymerase delta (10,11). Recently, RAD52 was identified as a key promoter of mitotic DNA synthesis in U2OS and HeLa cell lines due to its role in recruiting MUS81 in addition to its involvement in homologous recombination (HR) (11,31). Other HR proteins such as BRCA2 and RAD51 are dispensable for this process, as their absence enhances mitotic DNA synthesis in the presence/absence of Aph treatment (11,32,33). Sites of mitotic DNA synthesis are predominantly found at chromosome loci co-localizing with FANCD2 foci, which include specific loci known as common fragile sites (11,13,14,34,35). Importantly, mitotic DNA synthesis often generates gaps and breaks on metaphase chromosomes, promoting fragile site expression as a way to promote sister-chromatid separation (10,11,36). Despite tight co-localization of FANCD2 foci with sites of mitotic DNA synthesis, the role of FANCD2 in mitotic DNA synthesis is largely unknown in human cells.

In this study, we investigated the role of FANCD2 and its functional interplay with RAD52 in mitotic DNA synthesis using multiple human cancer and non-cancerous cell lines. A low

dose of Aph was used to universally induce mitotic DNA synthesis in all cell lines. Additionally, we discovered that partial inhibition of origin licensing works more effectively in cancer cell lines for the induction of mitotic DNA synthesis. In *cancer* cell lines (HCT116, H1299, U2OS, and HeLa), we found that FANCD2 and RAD52 act in parallel to support mitotic DNA synthesis regardless of how it was induced. In *non-cancerous* cell lines (hTERT-RPE1, BJ-5ta, HDFn, and IMR90), we observed that Aph-induced mitotic DNA synthesis predominantly depends on FANCD2, as RAD52 was dispensable for this process. These findings illustrate FANCD2 as a crucial regulator of mitotic DNA synthesis in human cells, thereby limiting the function of RAD52 as an additional driver to cancer cell lines.

Materials and Methods

Cell lines

The HCT116 cell line and its mutant derivatives (31,37) were generously provided by Drs. Eric Hendrickson and Alex Sobeck at the University of Minnesota. These lines have been authenticated by these researchers in house. The H1299, U2OS, HeLa, hTERT-RPE1, BJ-5ta, HDFn and IMR90 cell lines were purchased from ATCC between 2017–2018 and were cultured less than 8 weeks from frozen stocks of early passages (p2–4) for this study. All cell culture media were purchased from Sigma-Aldrich, supplemented with 10% fetal bovine serum (FBS, Atlanta Biologicals), and Penicillin-streptomycin (Thermo Fisher). Mycoplasma testing has not been performed on these cell lines. However, HCT116 and U2OS cells were cultured in McCoy's 5A (M8403) additionally supplemented with Plasmocin™ (mycoplasma elimination reagent, Invivogen) and GlutaMax™ (Thermo Fisher). H1299 cells were cultured in RPMI-1640 (R8758). RPE1 cells were cultured in DMEM/F12 (D6421) additionally supplemented with GlutaMax™ and 0.01% hygromycin B (Sigma). BJ cells were cultured in a 4:1 media mixture of DMEM (D6429) and Medium 199 (M4530) additionally supplemented with 0.01% hygromycin B. HDFn and Hela cells were cultured in DMEM (D6429). IMR90 cells were cultured in MEM (51416C) additionally supplemented with GlutaMax™.

Small-interfering RNA (siRNA) transfection

For immuno-fluorescence staining, cells were seeded on coverslips in wells of 6-well plates. Next day, cells were treated with siRNA using Lipofectamine™ iRNAMAX (Thermo Fisher) in Opti-MEM (Thermo Fisher) supplemented with 3% FBS. After 48 hrs of incubation with siRNA, cells were washed with phosphate-buffered saline (PBS) and cultured in fresh media containing 20 μM EdU (Lumiprobe) for 30 min before fixation with 10% formalin. When applicable, cells were cultured in the presence of 300 nM Aph, (150 nM for H1299, U2OS, HDFn and IMR90 cell lines) for the last 24 hrs of siRNA treatment. For immunoblots, cells were plated in 6 cm or 10 cm dishes for siRNA treatment to prepare whole cell lysates. Control siRNA, siRAD52-B, siORC1, and siFANCA-A/B were purchased from Dharmacon (D-001210–01, D-011760–01, D-003283–06, and D-019283–19/20 respectively). siRAD52-A was purchased from Qiagen (S103035123). siFANCD2-A (CAGAGUUUGCUUCACUCUCAUU) and -B (AACAGCCAUGGAUACACUUGA) (38) were synthesized by Dharmacon and Qiagen, respectively. siPOLD3 (s21045) was

purchased from Thermo Fisher. Unless specified, siRAD52-A (siR52A) and siFANCD2-A (siD2-A) were primarily used within the final concentrations of 30–60 nM in this study.

Immunofluorescent staining for FANCD2 foci and EdU spots

Fixed cells on coverslips were first subjected to a Click-Chemistry Reaction (20μM Biotin-Azide, 10mM sodium ascorbate, and 2mM $CuSO_4$ in PBS) at room temperature for one hour. After washing with PBS, cells were incubated with anti-FANCD2 (abcam ab108928; 1:250) and anti-phospho-Histone H3 at Ser10 (Cell Signaling 9706S; 1:200) antibodies in PBS containing 0.3% Triton X-100 and 1% BSA at 4°C overnight. Next day, cells were washed with PBS and incubated with Alexa Fluor 488 Streptavidin (Thermo Fisher S32354; 1:100), Alexa Fluor 350 anti-mouse (A11045; 1:100) and Alexa Fluor anti-rabbit (A31632; 1:1000) secondary antibodies at room temperature for one hour. Cells were washed with PBS, and coverslips were mounted on microscope slides with Prolong Gold™ anti-fade reagent (Thermo Fisher). EdU spots and FANCD2 foci were scored using a fluorescent microscope Axio Imager A1 (Zeiss). Experiments were performed three times to score at least 200 cells per treatment/genotype. Obtained data were combined to determine overall frequency of cells positive for EdU spots or >2 FANCD2 foci per genotype/treatment. Significance between frequencies among different genotypes/treatments was determined by a χ^2-test.

Immunoblotting

After trypsinization and centrifugation, cells were re-suspended in RIPA buffer (Sigma, R0278) supplemented with Pierce Protease Inhibitor (Thermo Fisher) for incubation on ice for 15 min. Cell lysates were then centrifuged at 10000 *g* for 20 min at 4°C to obtain supernatants. Prepared lysates were mixed with 4x NuPAGE® LDS Sample Buffer (Thermo Fisher) for separation on denaturing gradient gels (Novex Tris-Glycine 8–10% or Tris-Acetate 3–8%), which were transferred to Immobilon P membranes (Millipore). After blocking in 5% milk, membranes were incubated with primary antibodies at 4°C overnight. Subsequent incubation with horseradish peroxidase-conjugated rabbit secondary antibody (Jackson Labs) or mouse secondary antibody (Bio-Rad) occurred at room temperature for one hour. Protein bands were detected using Immobilon™ Western HRP Substrate (Millipore Sigma). Primary antibodies were used for immunoblotting at the following dilutions; anti-FANCD2 (ab108928, 1:2000), anti-tubulin (ab7291, 1:100,000), and anti-vinculin (ab18058, 1:100,000), anti-POLD3 (Bethyl A301–244AM, 1:1000) anti-RAD52 (Santa Cruz sc-365341, 1:750), anti-ORC1 (Sigma PLA0221, 1:2000), and anti-FANCA (Cell signaling 14657S, 1:1000)

Metaphase spreads

Cells plated in 6 cm dishes were cultured for two days in normal media or treated with siRNAs for 48 hrs before incubation with colcemid and 20 μM EdU for one hour. Cells were then trypsinized for fixation with a 3:1 ratio of methanol to glacial acetic acid to prepare metaphase spreads as previously described (39). Metaphase spreads were subjected to the Click-Chemistry Reaction as described above before staining with 4’,6-diamidino-2-phenylindole (DAPI). Metaphase chromosomes were scored for EdU spots and gaps/breaks using the fluorescent microscope. Experiments were performed three times to score at least

120 metaphase cells per treatment/genotype. The average number of EdU spots and gaps/breaks was determined for each genotype. Significance was determined by a *t*-test.

Cell proliferation/colony formation assays

After 48 hrs of incubation with siRNA, cells were trypsinized, and the number of live cells were counted by a trypan blue exclusion method using the Countess II Automated Cell Counter (Invitrogen). For colony formation assays, cells were then replated in 6 cm plates (600 cells/plate). Ten days later, colonies were fixed with 100% methanol, stained with Giemsa, and counted. Each assay was performed with triplicates per genotype/treatment and repeated three times. Significance between the average cell/colony numbers among different genotypes/treatments was determined by a *t*-test.

Results

Mitotic DNA synthesis is promoted not only by RAD52 but also by FANCD2 in HCT116 cells

We made use of an HCT116 mutant cell line lacking RAD52 (R52KO) (31) to understand the formation of EdU spots in the complete absence of RAD52 (see Fig. 1A). As spontaneous EdU spots are rarely observed in HCT116 cells regardless of genotype (Fig. 1C and Fig. 2B), we treated cells with Aph (300 nM) for 24 hrs followed by pulse-labeling with EdU for 30 min before fixation. We scored early M-phase (prophase to prometaphase) cells positive for phosphorylated Histone H3 at Serine 10 for the presence of EdU spots, which were almost always found at loci containing FANCD2 foci (Fig. 1B). As shown in Fig. 1C, the vast majority (94.5%±1.6) of parental HCT116 cells (refer to wildtype, WT) contained at least one EdU spot under this condition. In R52KO cells, the percentage of cells with EdU spots was slightly but significantly decreased to 78.5%±2.9, consistent with the promoting role of RAD52 in mitotic DNA synthesis (11). We noticed that the lack of RAD52 also caused a significant decrease in the number of cells positive for >2 FANCD2 foci (81.0% ±2.8) relative to WT cells (99.5%±0.5). Intrigued by this parallel decrease in FANCD2 foci in R52KO cells, we also used a HCT116 FANCD2 null line (D2KO)(37). Relative to WT cells, these cells formed Aph-induced EdU spots at a decreased frequency (82.5%±2.7), suggesting a role of FANCD2 in promoting mitotic DNA synthesis. As shown in Supplementary Fig. 1, we also depleted RAD52 or FANCD2 in WT cells using siRNAs, which consistently caused a significant decrease in the number of cells with Aph-induced EdU spots in both cases (87.0%±1.9 for siRAD52, 87.3%±1.9 for siFANCD2) relative to control siRNA (siC)-treated conditions (96.3%±1.1). Finally, we scored Aph-induced chromosome aberrations in WT, R52KO and D2KO cells. Regardless of genotype, nearly all (>98%) cells exhibited Aph-induced gaps and/or breaks on metaphase chromosomes (Fig. 1D), so we analyzed the number of gaps/breaks per cell among the genotypes (Fig. 1E). On average, 13.2±0.7 gaps/breaks were found per WT cell, and the majority (79.1%) were associated with EdU spots. Consistent with previous studies (11), the average number of gaps/breaks per cell was substantially decreased in R52KO cells (6.9±0.3), and only a small fraction of them were found at EdU spots (35.4%). Relative to WT cells, the average number of gaps/breaks per cell was significantly lower in D2KO cells (10.9±0.5), and the percentage of them at EdU spots was also decreased (65.9%). It should be noted that the observed decreases in gaps/breaks in R52KO and D2KO cells were also correlated with a lower

number of EdU spots per cell in these mutants compared to WT cells (Fig. 1F). Taken together, these findings reveal FANCD2 as a supporter of mitotic DNA synthesis in addition to RAD52 in HCT116 cells.

RAD52 and FANCD2 independently support the formation of EdU spots in HCT116 cells

As a next step, we wanted to test a functional interplay between RAD52 and FANCD2 in supporting mitotic DNA synthesis in HCT116 cells. However, we were unable to do so with Aph treatment due to poor viability of R52KO and D2KO cells when FANCD2 or RAD52 was additionally depleted. Previously, we and others reported that partial depletion of MCM4 or MCM5 induces EdU spots in mouse or human cells without the use of Aph (12,15). However, depletion of MCM4 strongly inhibited the proliferation of HCT116 as reported elsewhere (40), inducing EdU spots only in 12.7%±1.9 of surviving WT cells (Supplementary Fig. 2). Rather, we found that ORC1 depletion was far more efficient in inducing EdU spots in HCT116 cells, as the majority of WT cells were positive for EdU spots (70.3%±2.5, Fig. 2AB). Consistent with the data on Aph-induced EdU spots (Fig. 1), the lack of RAD52 or FANCD2 decreased the number of cells with EdU spots under this condition (34.6%±2.5 in R52KO, 51.3%±2.9 in D2KO, see Fig. 2B). Importantly, additional depletion of FANCD2 in R52KO cells substantially impaired the formation of EdU spots under ORC1 depletion (9.7%±1.7). Co-depletion of RAD52 with ORC1 in D2KO cells also had a similar inhibitory effect on the formation of EdU spots (32.0%±2.7). Moreover, co-depletion of RAD52 and FANCD2 caused a significant decrease of WT cells containing EdU spots under ORC1 depletion (45.3%±2.9). While it appears that RAD52 promotes mitotic DNA synthesis by supporting a full level of FANCD2 focus formation, these data collectively suggest that RAD52 and FANCD2 function independently of one another to promote EdU spot formation in HCT116 cells.

Multiple cancer cell lines also rely on both RAD52 and FANCD2 for mitotic DNA synthesis

Having found the dual regulation of mitotic DNA synthesis by RAD52 and FANCD2 in HCT116 cells, we wanted to test if this holds true for other cancer cell lines. In H1299 cells, a lung cancer cell line, Aph-induced EdU spots were observed in the vast majority of cells (93.9%±1.2) under siC-treated conditions (Fig. 3B left). As shown in Fig. 3AB, depletion of RAD52 by siR52-A caused a significant decrease in the number of cells containing EdU spots (76.5%±2.2). Depletion of FANCD2 by siD2-A caused a sharp reduction in the number of cells with EdU spots (47.3%±2.9). Co-depletion of RAD52 and FANCD2 by these siRNAs further decreased the number of cells with EdU spots than single depletion alone (28.6%±2.6). Note that we also observed a significant decrease in cells with EdU spots when RAD52 or FANCD2 was depleted by siR52-B or siD2-B, respectively. We next investigated the role of FANCA in mitotic DNA synthesis, as this protein is involved in the monoubiquitination of FANCD2 as a member of the Fanconi core complex (41). Depletion of FANCA (done independently using two different siRNAs; siFA-A and siFA-B) significantly reduced the number of cells with EdU spots at a level comparable to POLD3 depletion or lower (Fig. 3B, right). Therefore, FANCD2 and FANCA both promote mitotic DNA synthesis in H1299 cells. Unlike HCT116 cells, approximately one third of H1299 cells displayed basal EdU spots (30.9%±2.6) in siC-treated conditions. Upon ORC1 depletion, EdU spots were detected in nearly all cells (96.4%±1.1, Fig. 3CD). Induction of

EdU spots was significantly suppressed by co-depletion of RAD52 with ORC1 (72.3%±2.7). Co-depletion of FANCD2 and ORC1 substantially decreased the formation of EdU spots (22.7%±1.7). Co-depletion of RAD52, FANCD2 and ORC1 further decreased the number of cells with EdU spots (16.2%±2.1). These data are consistent with the dual regulation of mitotic DNA synthesis by FANCD2 and RAD52. We then examined U2OS and HeLa cells, which rely on RAD52 in promoting mitotic DNA synthesis (11). As shown in Supplementary Figs. 3 and 4, these cell lines also depend on FANCD2 for mitotic DNA synthesis in addition to RAD52 regardless of how it is induced.

Non-cancerous RPE1 cells rely on FANCD2 but not on RAD52 for EdU spot formation

We then extended our investigations to non-cancerous cell lines to understand if dual regulation of mitotic DNA synthesis is universal. We first used hTERT-RPE1 (RPE1), an hTERT-immortalized, noncancerous epithelial cell line. As shown in Fig. 4AB, Aph treatment induced EdU spots in the majority of siC-treated RPE1 cells (77.7%±1.8). Expectedly, depletion of POLD3 significantly decreased the number of cells with EdU spots compared to siC-treated conditions (54.9%±2.9). To our surprise, depletion of RAD52 (done independently using two different siRNAs) did not cause any significant change in the frequency of EdU positive cells (73.6%±2.4 for siR52-A, 77.0%±2.4 for siR52-B). However, FANCD2 depletion (also done independently using two different siRNAs) consistently caused a significant decrease in the number of cells with EdU spots relative to siC-treated conditions (56.5%±3.3 for siD2-A, 53.0%±2.9 for siD2-B). Co-depletion of RAD52 and FANCD2 also decreased the number of cells with EdU spots to levels seen in conditions of FANCD2 single depletion (53.6%±2.9). These data suggest that mitotic DNA synthesis in RPE1 cells depends primarily on FANCD2. To further verify this striking result, we constructed RAD52 deficient lines in RPE1 cells by genome editing (see Supplementary Methods). Consistent with RAD52 depletion by siRNAs, the absence of RAD52 in RPE1 cells did not cause any decrease in the number of cells with EdU spots (Fig. 4CD). Depletion of FANCD2 in R52KOB7, one of the R52KO lines constructed, resulted in a sharp decrease in cells with EdU spots. Moreover, depletion of FANCA also significantly impaired mitotic DNA synthesis in RPE1 cells. These findings strongly support that mitotic DNA synthesis in RPE1 cells is driven by these Fanconi proteins but not by RAD52. It should also be noted that a selective decrease in EdU-positive cells after FANCD2 depletion in RPE1 cells cannot be explained by a difference in cell cycle progression. Cell cycle profiles were very similar after RAD52 or FANCD2 depletion in RPE1 cells (Supplementary Fig. 5). In contrast to cancer cell lines, RPE1 cells were relatively insensitive to ORC1 depletion, as a small fraction of cells (23.0%±1.7) displayed EdU spots under this condition (Fig. 4EF). Consistently, co-depletion of RAD52 with ORC1 did not suppress the formation of EdU spots (22.0%±2.5). Interestingly, RAD52 depletion by itself slightly increased the number of cells positive for EdU spots as well as FANCD2 foci.

As it appears that RAD52 is dispensable for mitotic DNA synthesis in RPE1 cells, we tested the role of BRCA2 in induction of EdU spots. As reported previously (11,32,33), depletion of BRCA2 (done independently using two different siRNAs) induced EdU spots in ~50% of RPE1 cells, which was effectively suppressed by co-depletion of POLD3 (Supplementary Fig. 6AB). EdU spots induced under BRCA2 depletion were also associated with

chromosome aberrations (Supplementary Fig. 6C). Therefore, EdU spots formed under this condition displayed the features of mitotic DNA synthesis. These findings indicate that RAD52 and BRCA2 are both dispensable for mitotic DNA synthesis in RPE1 cells.

Depletion of RAD52 increases EdU spot formation in non-cancerous fibroblasts

To exclude the possibility that RPE1 cells are an exceptional cell line which does not require RAD52 for mitotic DNA synthesis, we next examined BJ-5ta (BJ) cells, an hTERT-immortalized non-cancerous fibroblast cell line (Fig. 5). Following Aph treatment, approximately half of BJ cells displayed EdU spots (48.0%±2.9). Unexpectedly, depletion of RAD52 by siR52-A caused a 1.8-fold increase in cells with EdU spots (87.3%±1.9, Fig. 5AB). While RAD52 depletion by siR52-B did not change the percentage of cells positive for EdU spots (46.7%±2.9, Fig. 5AB), it increased the number of cells with ≥20 EdU spots (12%) relative to siC-treated conditions (0.67%, Fig. 5C, left). Overall, RAD52 depletion enhanced EdU spot formation in BJ cells, which accompanied a significant increase in the fraction of cells with ≥20 FANCD2 foci (45.3% for siR52-A, 70.0% for siR52-B, relative to 34.3% for siC, Fig. 5C right). As seen in RPE1 cells, depletion of FANCD2 decreased the number of cells positive for EdU spots (36.3%±2.8 for siD2-A, 23.5%±2.5 for siD2-B). Co-depletion of RAD52 and FANCD2 significantly suppressed the formation of EdU spots (32.3%±2.7 for siR52-A+siD2-A, 33.7%±2.7 for siR52-B+siD2-A), suggesting that FANCD2 is a dominant factor to support mitotic DNA synthesis in BJ cells. Under ORC1 depletion, BJ cells with EdU spots were very rare (3.0%±0.98), although FANCD2 focus formation was greatly enhanced relative to siC-treated conditions (Fig. 5B right). We further tested HDFn and IMR90, primary fibroblast cell lines (Fig. 6). Again, RAD52 depletion by siR52-A caused a significant increase in the number of cells positive for Aph-induced EdU spots (60.0%±2.4 for HDFn, 67.7%±3.2 for IMR90) from siC-treated conditions (46.0% ±2.9 for HDFn, 41.8%±3.2 for IMR90). When siR52-B was used, Aph-induced EdU spots were also significantly increased in HDFn cells (52.0%±2.9). Therefore, RAD52 may have an inhibitory role in mitotic DNA synthesis in fibroblasts. Depletion of FANCD2 significantly decreased the number of cells with EdU spots (19.0%±2.2 for HDFn, 34.6% ±3.5 for IMR90), suggesting FANCD2 as a dominant player in supporting mitotic DNA synthesis in these cells. In these cell lines, ORC1 depletion had very little effect on the induction of EdU spots (9.0%±1.7 for HDFn, 4.3%±1.2 for IMR90). These data suggest that ORC1 depletion is far more effective at inducing mitotic DNA synthesis in cancer cells than non-cancerous cells. This may be attributed, partially if not all, to the highly up-regulated expression of ORC1 in cancer cell lines relative to non-cancerous cell lines (Fig.7A)(42).

Co-depletion of RAD52 and ORC1 selectively impairs the proliferation of cancer cells

RAD52 now emerges as an attractive target for cancer therapies given its role in mitotic DNA synthesis (11). To enhance the efficacy of this strategy, we exploited ORC1 depletion to induce mitotic DNA synthesis preferentially in cancer cells. In a short-term assay to determine cell numbers (Fig. 7B, top), HCT116 R52KO cells (as well as D2KO cells) were found to be less proliferative relative to WT HCT116 cells even in siC-treated conditions (31,37). ORC1 depletion further impaired the proliferation of these cells. Co-depletion of RAD52 and ORC1 also impaired the proliferation of U2OS cells but not of RPE1 or BJ cells relative to siC-treated conditions (Fig. 7C). In a colony forming assay (Fig. 7B, bottom), the

less proliferative nature of HCT116 R52KO cells was more evident particularly after ORC1 depletion. Co-depletion of RAD52 and ORC1 also substantially inhibited the colony forming abilities of H1299 and U2OS cells compared to siC-treated conditions (Fig. 7D). We could not perform the colony forming assay on non-cancerous cell lines, because these cells did not form distinct, scorable colonies. Overall, these data support that co-targeting RAD52 and ORC1 selectively impairs the proliferation of cancer cells.

Discussion

In this study, we demonstrated that FANCD2 supports mitotic DNA synthesis along with RAD52 in cancer cell lines. Moreover, our data consistently indicate that mitotic DNA synthesis in non-cancerous cell lines predominantly depends on FANCD2. Unexpectedly, RAD52 had little effect on mitotic DNA synthesis in RPE1 cells. In the fibroblast cell lines, it appears that RAD52 suppresses mitotic DNA synthesis, as its depletion significantly enhanced the formation of EdU spots. Collectively, we propose models (Fig. 7E) in which FANCD2 acts as a fundamental player in mitotic DNA synthesis in human cells. Recent studies identified a RAD52-independent mechanism for DNA synthesis at telomeres during the G2/M phases in cancer cells (43,44). Since this unusual timing of DNA synthesis at telomeres displays mechanistic similarities with mitotic DNA synthesis, it will be intriguing to find out if this new mechanism also depends on FANCD2. Given our finding on the involvement of FANCA in mitotic DNA synthesis (Figs 3 and 4), it is likely that the Fanconi core complex and FANCD2 coordinately regulate this process independently of BRCA2/RAD51 (FANCD1/FANCR). In this context, it will be important to understand the underlying mechanism with respect to the human genetic disorder Fanconi anemia. In contrast, we previously reported that FANCC was dispensable for EdU spot formation in mice (12), suggesting the possibility that mitotic DNA synthesis operates differently between these species. It may be possible that mitotic DNA synthesis in mice primarily depends on RAD52 or unknown factors. These possibilities should be addressed in future studies. Our findings suggest that the role of RAD52 in mitotic DNA synthesis is restricted to cancer cells. Given the highly up-regulated expression of RAD52 in cancer cells (Fig. 7A), we speculate that RAD52 may acquire a role as an additional promoter of mitotic DNA synthesis during cancer development. This may allow for cancer cells to perform an “upgraded” form of mitotic DNA synthesis, which may help them cope with replication stress to sustain their survival and proliferation.

While RAD52 depletion reproducibly caused a significant inhibition of EdU spot formation in cancer cells, its effect on FANCD2 focus formation was far from uniform among the cancer cell lines used in this study. In HCT116 cells, the absence/depletion of RAD52 invariably resulted in a decline in the number of FANCD2 foci (Figs. 1 and 2, and Supplementary Fig. 1). In H1299 cells, RAD52 depletion had either no effect or impaired FANCD2 focus formation (Fig. 3). In U2OS and HeLa cells, we observed complicated bimodal forms of FANCD2 focus formation (see Supplementary Figs. 3 and 4). While such differences may be attributed to cancer types, mutations/deficiencies each cancer line harbors, and/or their intrinsic genetic make-ups, we do not have a feasible explanation for it at this time. Whatever the effect of RAD52 depletion on FANCD2 focus formation would be, our data inherently point out that RAD52 and FANCD2 function independently in

mitotic DNA synthesis in the cancer cell lines we tested. On the other hand, RAD52 depletion consistently enhanced the formation of FANCD2 foci and EdU spots in the fibroblast cell lines. Even in RPE1 cells, we found that depletion/lack of RAD52 increases the number of FANCD2 foci per cell (see R52KOD8 in Fig.4D).

Without Aph treatment, EdU spots were rarely observed in non-cancerous cell lines. This was also the case for HCT116 cells. However, other cancer cell lines (in particular H1299 cells) had relatively high basal levels of EdU spots along with an increased number of FANCD2 foci. As shown for DNA synthesis at telomeres during G/M phases, the status of p53 may play a role for high basal levels of EdU spots (45). While Aph is a non-selective inducer of mitotic DNA synthesis, depletion of ORC1 induced EdU spots preferentially in cancer cells. This is consistent with the idea that cancer cells rely heavily on dormant origins to resolve stalled replication forks to better cope with intrinsic replication stress they may harbor. In fact, depletion of ORC or MCM proteins cause a significant loss of dormant origins (26,27,46), which makes cancer cells far less viable and proliferative relative to non-cancerous cells (42,47). In this context, a loss of dormant origins is expected to cause the accumulation of late replication intermediates especially in cancer cells, which are most likely resolved by mitotic DNA synthesis. Supported by our data (Fig. 7B–D), inhibition of mitotic DNA synthesis by targeting RAD52 under such conditions may provide a chance to selectively impair the proliferation of cancer cells. For this purpose, we think that ORC is a better target, as a chronic reduction of MCM causes tumors in mice (48,49). On the other hand, defects in ORC are associated with Meier-Gorlin syndrome, a primordial dwarfism which has no known increased risks of cancer (50).

Supplementary Material

Refer to Web version on PubMed Central for supplementary material.

Acknowledgments

This work is supported by grants from the National Institutes of Health (NIH) to N. Shima primarily by NCI R03 CA227215 and partially by NIEHS R21 ES027062. We thank Drs. Eric Hendrickson and Alex Sobeck at the University of Minnesota for HCT116 cell lines. We also appreciate Madison Duffy, Anika Tella and Madeleine Hinojos for their technical help. This work was supported in part by NIH P30 CA77598 utilizing the following; Masonic Cancer Center, University of Minnesota Shared Resource: Genome Engineering Shared Resource (GESR).

References

1. Macheret M, Halazonetis TD. DNA replication stress as a hallmark of cancer. Annu Rev Pathol 2015;10:425–48. [PubMed: 25621662]
2. Gaillard H, García-Muse T, Aguilera A. Replication stress and cancer. Nat Rev Cancer 2015;15:276–89. [PubMed: 25907220]
3. Bartkova J, Rezaei N, Liontos M, Karakaidos P, Kletsas D, Issaeva N, et al. Oncogene-induced senescence is part of the tumorigenesis barrier imposed by DNA damage checkpoints. Nature 2006;444:633–7. [PubMed: 17136093]
4. Di Micco R, Fumagalli M, Cicalese A, Piccinin S, Gasparini P, Luise C, et al. Oncogene-induced senescence is a DNA damage response triggered by DNA hyper-replication. Nature 2006;444:638–42. [PubMed: 17136094]

5. Bartkova J, Horejsi Z, Koed K, Kramer A, Tort F, Zieger K, et al. DNA damage response as a candidate anti-cancer barrier in early human tumorigenesis. Nature 2005;434:864–70. [PubMed: 15829956]
6. Gorgoulis VG, Vassiliou LV, Karakaidos P, Zacharatos P, Kotsinas A, Liloglou T, et al. Activation of the DNA damage checkpoint and genomic instability in human precancerous lesions. Nature 2005;434:907–13. [PubMed: 15829965]
7. Halazonetis TD, Gorgoulis VG, Bartek J. An oncogene-induced DNA damage model for cancer development. Science 2008;319:1352–5. [PubMed: 18323444]
8. Negrini S, Gorgoulis VG, Halazonetis TD. Genomic instability--an evolving hallmark of cancer. Nat Rev Mol Cell Biol 2010;11:220–8. [PubMed: 20177397]
9. Bartek J, Bartkova J, Lukas J. DNA damage signalling guards against activated oncogenes and tumour progression. Oncogene 2007;26:7773–9. [PubMed: 18066090]
10. Minocherhomji S, Ying S, Bjerregaard VA, Bursomanno S, Aleliunaite A, Wu W, et al. Replication stress activates DNA repair synthesis in mitosis. Nature 2015;528:286–90. [PubMed: 26633632]
11. Bhowmick R, Minocherhomji S, Hickson ID. RAD52 Facilitates Mitotic DNA Synthesis Following Replication Stress. Mol Cell 2016;64:1117–26. [PubMed: 27984745]
12. Luebben SW, Kawabata T, Johnson CS, O'Sullivan MG, Shima N. A concomitant loss of dormant origins and FANCC exacerbates genome instability by impairing DNA replication fork progression. Nucleic Acids Res 2014;42:5605–15. [PubMed: 24589582]
13. Bergoglio V, Boyer AS, Walsh E, Naim V, Legube G, Lee MY, et al. DNA synthesis by Pol η promotes fragile site stability by preventing under-replicated DNA in mitosis. J Cell Biol 2013;201:395–408. [PubMed: 23609533]
14. Naim V, Wilhelm T, Debatisse M, Rosselli F. ERCC1 and MUS81-EME1 promote sister chromatid separation by processing late replication intermediates at common fragile sites during mitosis. Nat Cell Biol 2013;15:1008–15. [PubMed: 23811686]
15. Moreno A, Carrington JT, Albergante L, Al Mamun M, Haagensen EJ, Komseli ES, et al. Unreplicated DNA remaining from unperturbed S phases passes through mitosis for resolution in daughter cells. Proc Natl Acad Sci U S A 2016;113:E5757–64. [PubMed: 27516545]
16. Siddiqui K, On KF, Diffley JF. Regulating DNA replication in eukarya. Cold Spring Harb Perspect Biol 2013;5 a012930. [PubMed: 23838438]
17. Parker MW, Botchan MR, Berger JM. Mechanisms and regulation of DNA replication initiation in eukaryotes. Crit Rev Biochem Mol Biol 2017:1–41.
18. Miotto B, Ji Z, Struhl K. Selectivity of ORC binding sites and the relation to replication timing, fragile sites, and deletions in cancers. Proc Natl Acad Sci U S A 2016;113:E4810–9. [PubMed: 27436900]
19. Evrin C, Clarke P, Zech J, Lurz R, Sun J, Uhle S, et al. A double-hexameric MCM2–7 complex is loaded onto origin DNA during licensing of eukaryotic DNA replication. Proc Natl Acad Sci U S A 2009;106:20240–5. [PubMed: 19910535]
20. Remus D, Beuron F, Tolun G, Griffith JD, Morris EP, Diffley JF. Concerted loading of Mcm2–7 double hexamers around DNA during DNA replication origin licensing. Cell 2009;139:719–30. [PubMed: 19896182]
21. Gambus A, Khoudoli GA, Jones RC, Blow JJ. MCM2–7 form double hexamers at licensed origins in Xenopus egg extract. J Biol Chem 2011;286:11855–64. [PubMed: 21282109]
22. Deegan TD, Diffley JF. MCM: one ring to rule them all. Curr Opin Struct Biol 2016;37:145–51. [PubMed: 26866665]
23. Moyer SE, Lewis PW, Botchan MR. Isolation of the Cdc45/Mcm2–7/GINS (CMG) complex, a candidate for the eukaryotic DNA replication fork helicase. Proc Natl Acad Sci U S A 2006;103:10236–41. [PubMed: 16798881]
24. Gambus A, Jones RC, Sanchez-Diaz A, Kanemaki M, van Deursen F, Edmondson RD, et al. GINS maintains association of Cdc45 with MCM in replisome progression complexes at eukaryotic DNA replication forks. Nat Cell Biol 2006;8:358–66. [PubMed: 16531994]
25. Pacek M, Tutter AV, Kubota Y, Takisawa H, Walter JC. Localization of MCM2–7, Cdc45, and GINS to the site of DNA unwinding during eukaryotic DNA replication. Mol Cell 2006;21:581–7. [PubMed: 16483939]

26. Ge XQ, Jackson DA, Blow JJ. Dormant origins licensed by excess Mcm2–7 are required for human cells to survive replicative stress. Genes Dev 2007;21:3331–41. [PubMed: 18079179]
27. Ibarra A, Schwob E, Mendez J. Excess MCM proteins protect human cells from replicative stress by licensing backup origins of replication. Proc Natl Acad Sci U S A 2008;105:8956–61. [PubMed: 18579778]
28. Ha SA, Shin SM, Namkoong H, Lee H, Cho GW, Hur SY, et al. Cancer-associated expression of minichromosome maintenance 3 gene in several human cancers and its involvement in tumorigenesis. Clin Cancer Res 2004;10:8386–95. [PubMed: 15623617]
29. Ishimi Y, Okayasu I, Kato C, Kwon HJ, Kimura H, Yamada K, et al. Enhanced expression of Mcm proteins in cancer cells derived from uterine cervix. Eur J Biochem 2003;270:1089–101. [PubMed: 12631269]
30. McNairn AJ, Gilbert DM. Overexpression of ORC subunits and increased ORC-chromatin association in transformed mammalian cells. J Cell Biochem 2005;96:879–87. [PubMed: 16163736]
31. Kan Y, Batada NN, Hendrickson EA. Human somatic cells deficient for RAD52 are impaired for viral integration and compromised for most aspects of homology-directed repair. DNA Repair (Amst) 2017;55:64–75. [PubMed: 28549257]
32. Feng W, Jasin M. BRCA2 suppresses replication stress-induced mitotic and G1 abnormalities through homologous recombination. Nat Commun 2017;8:525. [PubMed: 28904335]
33. Lai X, Broderick R, Bergoglio V, Zimmer J, Badie S, Niedzwiedz W, et al. MUS81 nuclease activity is essential for replication stress tolerance and chromosome segregation in BRCA2-deficient cells. Nat Commun 2017;8:15983. [PubMed: 28714477]
34. Chan KL, Palmai-Pallag T, Ying S, Hickson ID. Replication stress induces sister-chromatid bridging at fragile site loci in mitosis. Nat Cell Biol 2009;11:753–60. [PubMed: 19465922]
35. Naim V, Rosselli F. The FANC pathway and BLM collaborate during mitosis to prevent micro-nucleation and chromosome abnormalities. Nat Cell Biol 2009;11:761–8. [PubMed: 19465921]
36. Ying S, Minocherhomji S, Chan KL, Palmai-Pallag T, Chu WK, Wass T, et al. MUS81 promotes common fragile site expression. Nat Cell Biol 2013;15:1001–7. [PubMed: 23811685]
37. Thompson EL, Yeo JE, Lee EA, Kan Y, Raghunandan M, Wiek C, et al. FANCI and FANCD2 have common as well as independent functions during the cellular replication stress response. Nucleic Acids Res 2017;45:11837–57. [PubMed: 29059323]
38. Chen YH, Jones MJ, Yin Y, Crist SB, Colnaghi L, Sims RJ, et al. ATR-mediated phosphorylation of FANCI regulates dormant origin firing in response to replication stress. Mol Cell 2015;58:323–38. [PubMed: 25843623]
39. Luebben SW, Kawabata T, Akre MK, Lee WL, Johnson CS, O'Sullivan MG, et al. Helq acts in parallel to Fancc to suppress replication-associated genome instability. Nucleic Acids Res 2013;41:10283–97. [PubMed: 24005041]
40. Liu Y, He G, Wang Y, Guan X, Pang X, Zhang B. MCM-2 is a therapeutic target of Trichostatin A in colon cancer cells. Toxicol Lett 2013;221:23–30. [PubMed: 23770000]
41. Garcia-Higuera I, Taniguchi T, Ganesan S, Meyn MS, Timmers C, Hejna J, et al. Interaction of the Fanconi anemia proteins and BRCA1 in a common pathway. Mol Cell 2001;7:249–62 [PubMed: 11239454]
42. Zimmerman KM, Jones RM, Petermann E, Jeggo PA. Diminished origin-licensing capacity specifically sensitizes tumor cells to replication stress. Mol Cancer Res 2013;11:370–80. [PubMed: 23364533]
43. Verma P, Dilley RL, Zhang T, Gyparaki MT, Li Y, Greenberg RA. RAD52 and SLX4 act nonepistatically to ensure telomere stability during alternative telomere lengthening. Genes Dev 2019;33:221–35. [PubMed: 30692206]
44. Zhang JM, Yadav T, Ouyang J, Lan L, Zou L. Alternative Lengthening of Telomeres through Two Distinct Break-Induced Replication Pathways. Cell Rep 2019;26:955–68.e3. [PubMed: 30673617]
45. Min J, Wright WE, Shay JW. Alternative Lengthening of Telomeres Mediated by Mitotic DNA Synthesis Engages Break-Induced Replication Processes. Mol Cell Biol 2017;37 (20) e00226–17. [PubMed: 28760773]

46. Kawabata T, Luebben SW, Yamaguchi S, Ilves I, Matise I, Buske T, et al. Stalled fork rescue via dormant replication origins in unchallenged S phase promotes proper chromosome segregation and tumor suppression. Mol Cell 2011;41:543–53. [PubMed: 21362550]

47. Bryant VL, Elias RM, McCarthy SM, Yeatman TJ, Alexandrow MG. Suppression of Reserve MCM Complexes Chemosensitizes to Gemcitabine and 5-Fluorouracil. Mol Cancer Res 2015;13:1296–305. [PubMed: 26063742]

48. Shima N, Alcaraz A, Liachko I, Buske TR, Andrews CA, Munroe RJ, et al. A viable allele of Mcm4 causes chromosome instability and mammary adenocarcinomas in mice. Nat Genet 2007;39:93–8. [PubMed: 17143284]

49. Pruitt SC, Bailey KJ, Freeland A. Reduced Mcm2 Expression Results in Severe Stem/Progenitor Cell Deficiency and Cancer. Stem Cells 2007;25:3121–32. [PubMed: 17717065]

50. Bicknell LS, Walker S, Klingseisen A, Stiff T, Leitch A, Kerzendorfer C, et al. Mutations in ORC1, encoding the largest subunit of the origin recognition complex, cause microcephalic primordial dwarfism resembling Meier-Gorlin syndrome. Nat Genet 2011;43:350–5. [PubMed: 21358633]

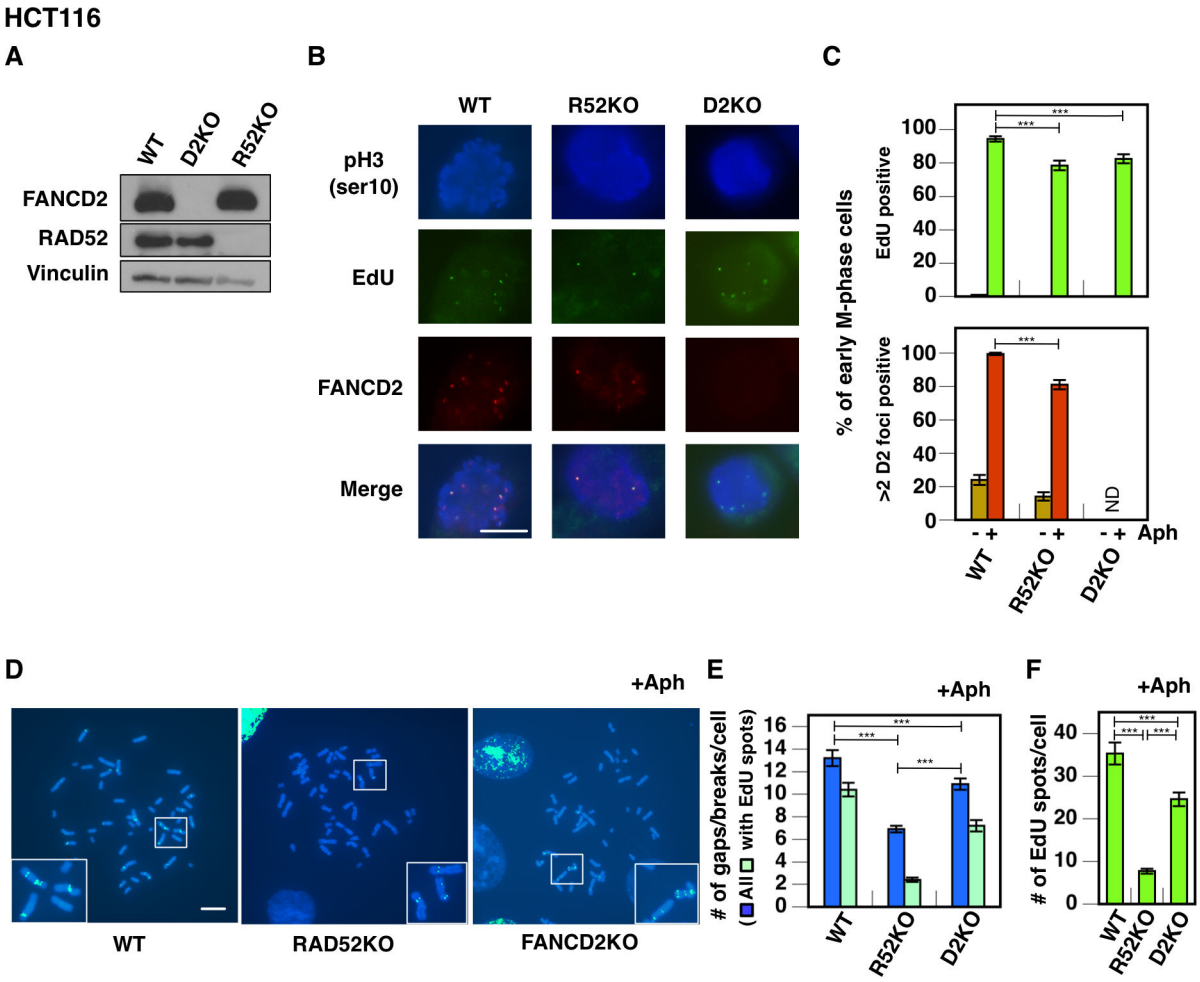

Figure 1. FANCD2 promotes mitotic DNA synthesis in addition to RAD52 in HCT116 cells.

A. Immunoblotting to confirm the lack of FANCD2 and RAD52 in respective mutant lines (D2KO and R52KO) along with expression levels of these proteins in parental wild-type (WT) cells. Vinculin was used as a loading control. **B**. Representative images of phospho-H3 stained nuclei/chromosomes (blue), EdU spots (green), and FANCD2 (red) foci are displayed for each genotype. **C**. Percentage of early M-phase (prophase to prometaphase) cells positive for EdU spots (top) or >2 FANCD2 foci (bottom) in the presence/absence of Aph treatment for each genotype. **D**. Representative images of metaphase spreads that display Aph-induced EdU spots and/or gaps/breaks in each genotype. **E**. The average number of gaps/breaks for each genotype and those found at EdU spots per cell. **F**. The average number of EdU spots for each genotype. Error bars indicate standard deviations of respective frequencies in **C** and standard errors of means in **E** and **F**, respectively. *** indicates $p<0.001$ by a χ^2-test in **C** and by a *t*-test in **E** and **F**, respectively. Bars in microscope images in **B** and **D** indicate 10 μm. ND; none detected.

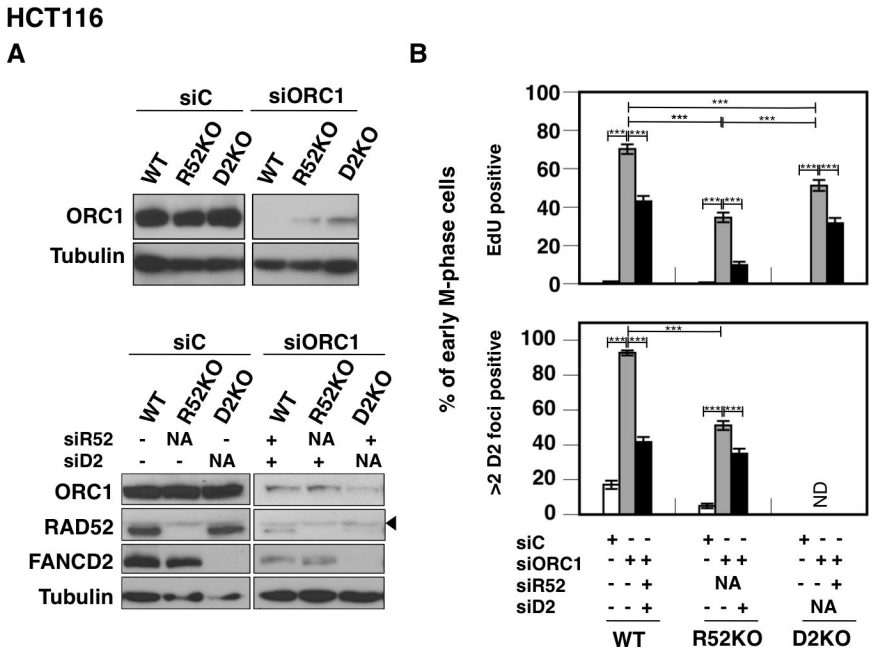

Figure 2. FANCD2 and RAD52 act in parallel in supporting EdU spot formation under ORC1 depletion in HCT116 cells.

A. Immunoblotting to show depletion of ORC1 (top/bottom) in all genotypes and additional depletion of RAD52 and/or FANCD2 (bottom) in respective HCT116 genotypes. Tubulin was used as a loading control. A filled triangle indicates a non-specific band detected by the RAD52 antibody. **B**. Percentage of early M-phase cells positive for EdU spots (top) or >2 FANCD2 foci (bottom) after ORC1 depletion in combination with RAD52 and/or FANCD2 depletion. Error bars indicate standard deviations of respective frequencies. *** indicates $p<0.001$ by a χ^2- test. ND; none detected. NA; not applicable.

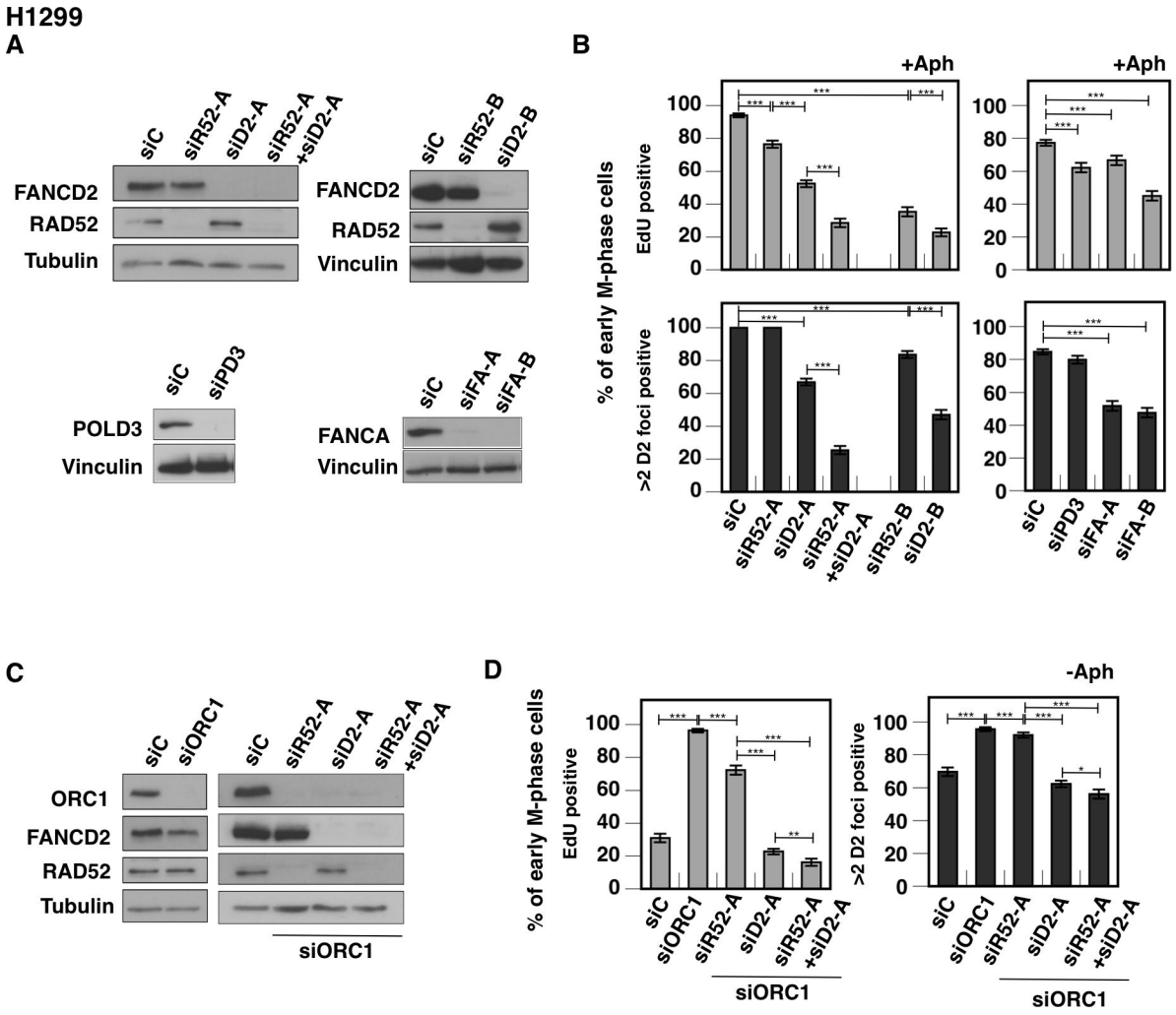

Figure 3. FANCD2 and RAD52 both support the formation of APH- and siORC1-induced EdU spots in H1299 cells.

A. Immunoblotting (top) to show depletion of RAD52 and/or FANCD2. Immunoblotting (bottom) to show single depletion of POLD3 (left) or FANCA (right). **B**. Percentage of early M-phase cells positive for EdU spots (top) or >2 FANCD2 foci (bottom) per siRNA treatment after Aph treatment. **C**. Immunoblotting to show single depletion of ORC (left), and co-depletion of RAD52 and/or FANCD2 with ORC1 (right). **D**. Percentage of early M phase cells positive for EdU spots (left) or >2 FANCD2 foci (right) per siRNA treatment. In **B** and **D**, error bars indicate standard deviations of respective frequencies. *. **. and *** indicate $p<0.05$, $p<0.01$, and $p<0.001$ by a χ^2- test, respectively.

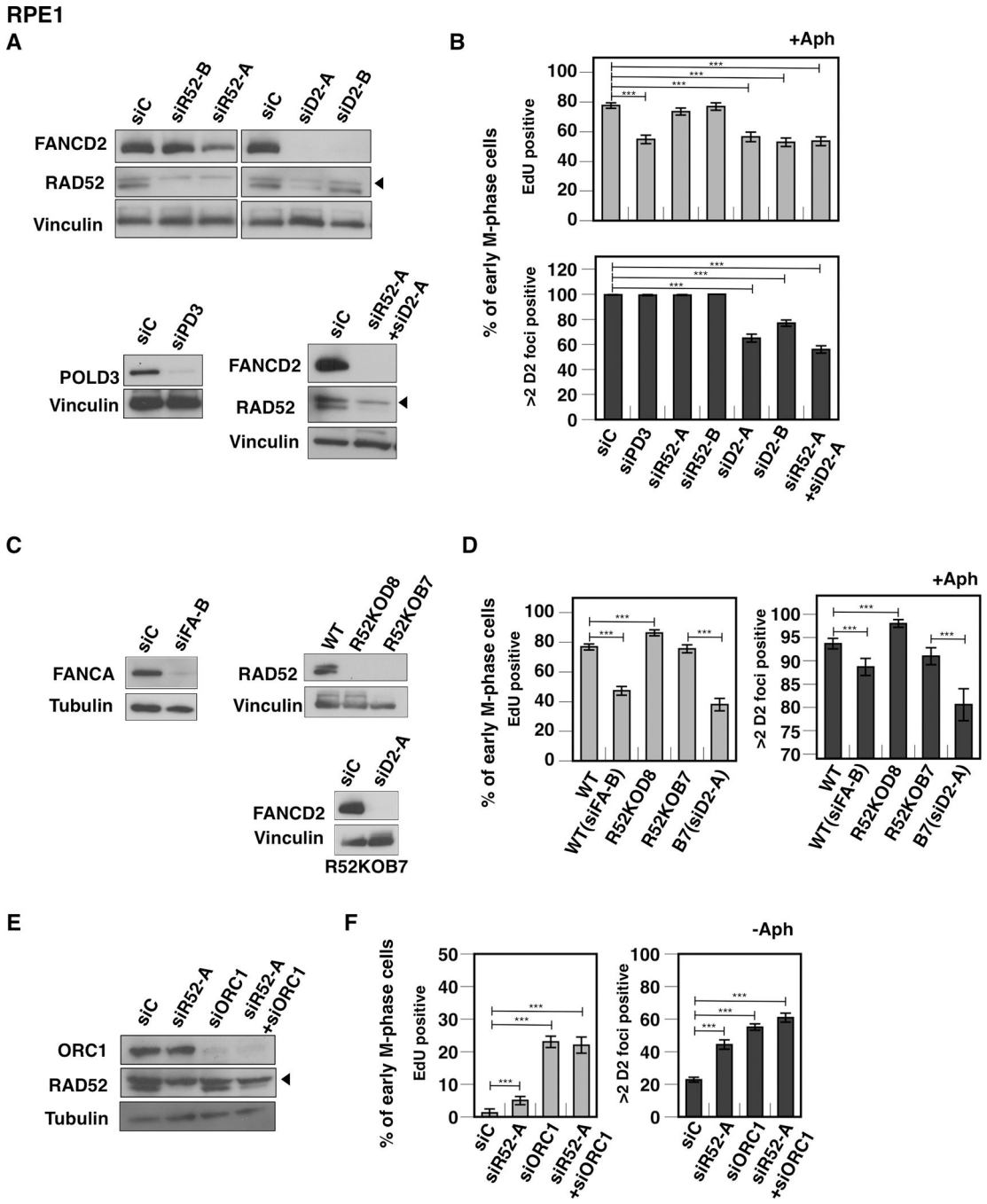

Figure 4. FANCD2 but not RAD52 supports the formation of EdU spots in RPE1 cells.

A. Immunoblotting to show single depletion of RAD52 (top left) or FANCD2 (top right), POLD3 (bottom left), and double depletion of FANCD2 and RAD52 (bottom right). **B**. Percentage of early M-phase cells positive for EdU spots (top) or >2 FANCD2 foci (bottom) per siRNA treatment group after APH treatment. **C**. Immunoblotting to show depletion of FANCA (top left), the lack of RAD52 (top right), and depletion of FANCD2 in R52KOB7 (bottom). **D**. Percentage of early M-phase cells positive for EdU spots (left) or >2 FANCD2 foci (right) per siRNA treatment/genotype group. **E**. Immunoblotting to show single

depletion of RAD52 and ORC1 and double depletion of RAD52 and ORC1. **F**. Percentage of early M-phase cells positive for EdU spots (left) or >2 FANCD2 foci (right) per siRNA treatment group. In **A** and **E**, filled triangles indicate a non-specific band detected by the RAD52 antibody. In **B**, **D** and **F**, error bars indicate standard deviations of respective frequencies. *** indicates $p<0.001$ by a χ^2- test.

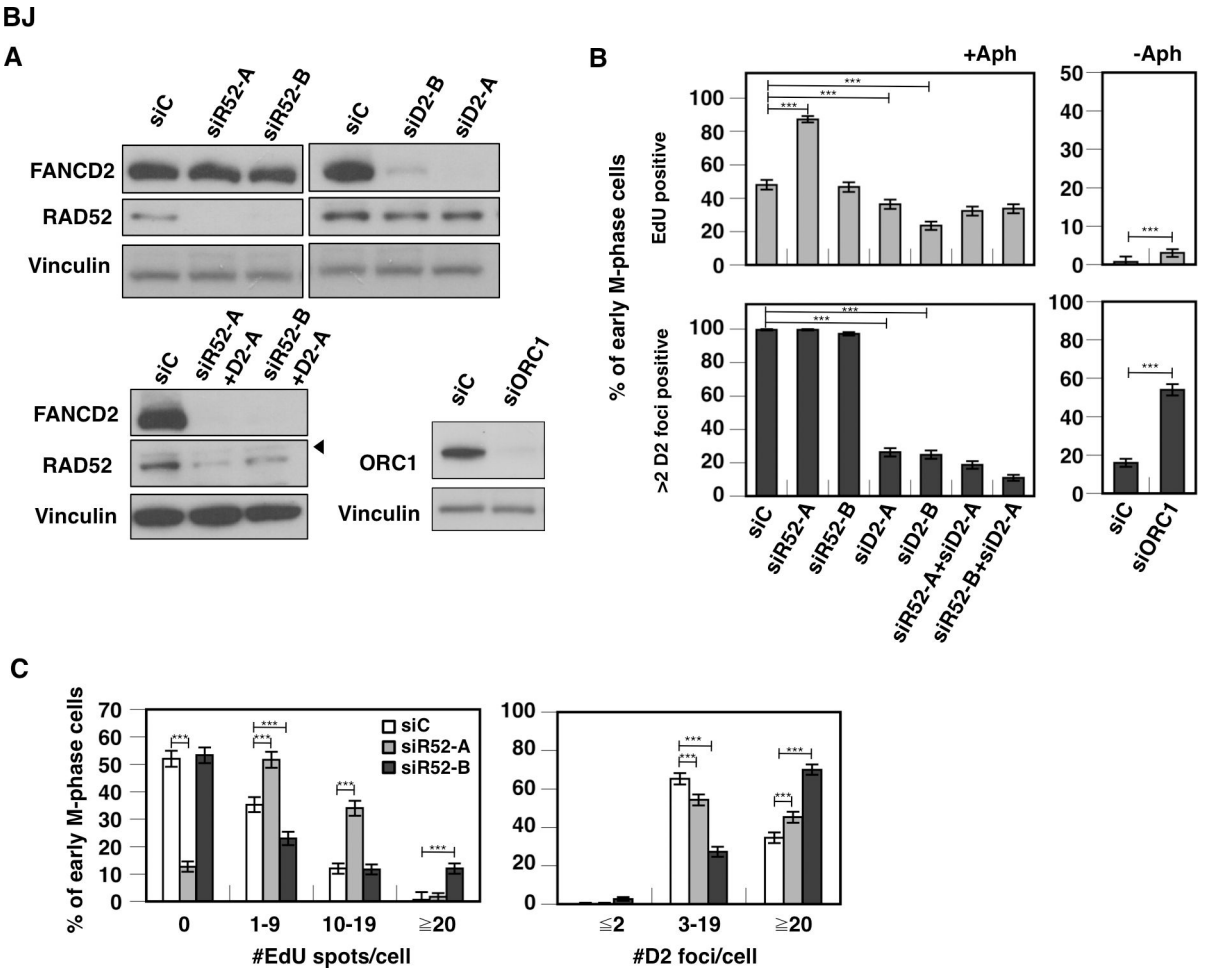

Figure 5. BJ cells rely on FANCD2 but not on RAD52 for EdU spot formation.

A. Immunoblotting to show single depletion of RAD52 (top left), FANCD2 (top right) or ORC1 (bottom right), and double depletion of FANCD2 and RAD52 (bottom left). **B**. Percentage of early M-phase cells positive for EdU spots (top) or >2 FANCD2 foci (bottom) per siRNA treatment group in the presence/absence of Aph treatment. **C**. Distribution of cells having respective ranges of EdU spots (left) and FANCD2 foci (right) per cell for each siRNA treatment. In **A**, a filled triangle indicates a non-specific band detected by the RAD52 antibody. In **B** and **C**, error bars indicate standard deviations of respective frequencies. *** indicates $p<0.001$ by a χ^2- test.

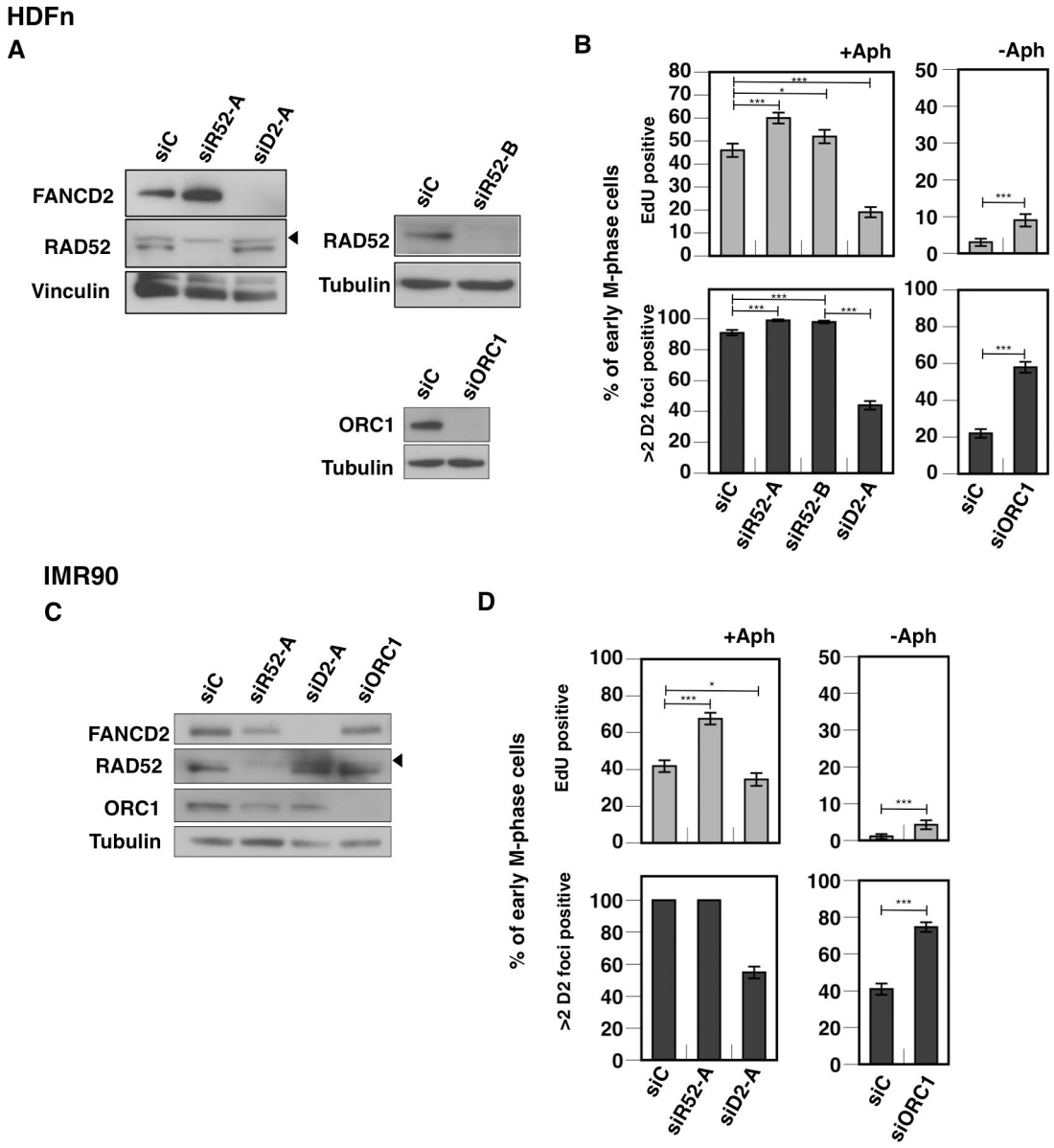

Figure 6. EdU spot formation is impaired by FANCD2 depletion but enhanced by RAD52 depletion in primary HDFn and IMR90 cells.

A. C. Immunoblotting to show single depletion of RAD52, FANCD2 or ORC1 in HDFn (A) and IMR90 cells (**C**). **B. D.** Percentage of early M-phase cells positive for EdU spots (top) or >2 FANCD2 foci (bottom) per siRNA treatment group in the presence/absence of Aph treatment for HDFn (**B**) and IMR 90 (**D**) cells. In **A** and **C**, filled triangles indicate a non-specific band detected by the RAD52 antibody. In **B** and **D**, error bars indicate standard deviations of respective frequencies. * and *** indicate $p<0.05$ and $p<0.001$ by a χ^2- test, respectively.

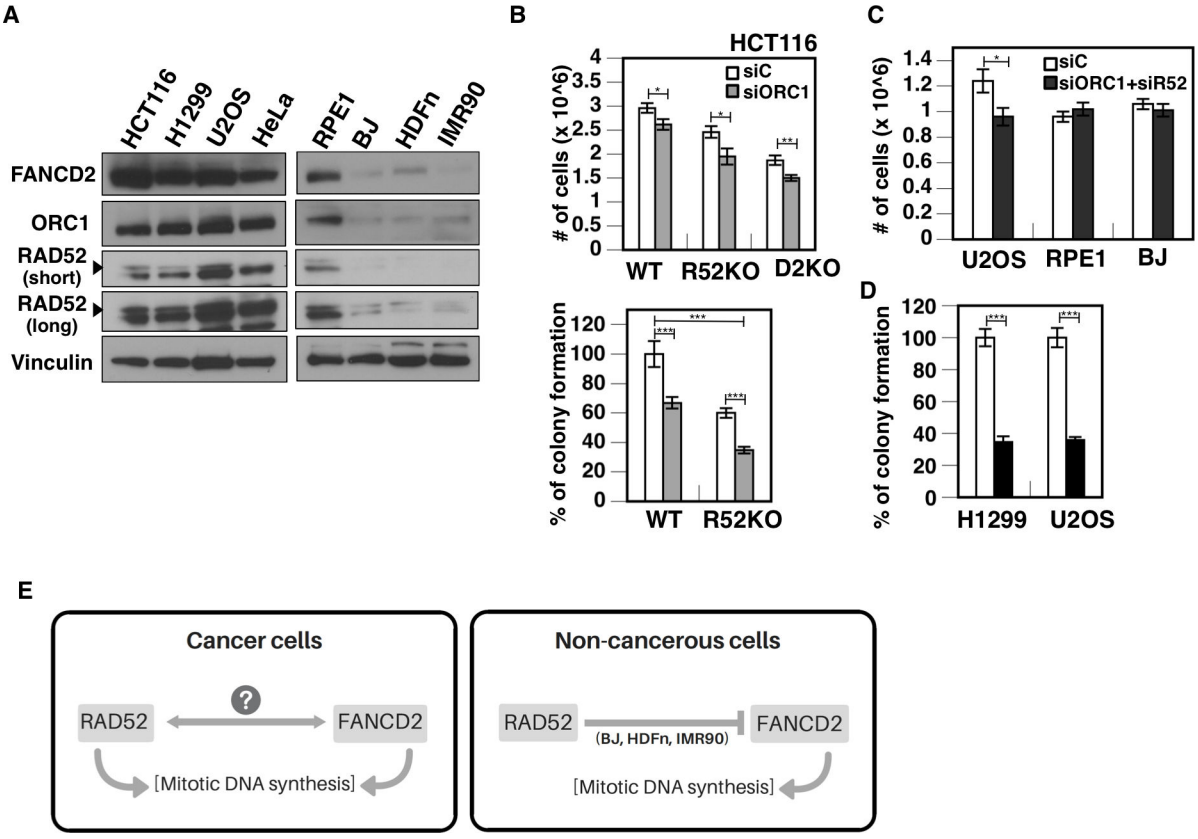

Figure 7. Co-depletion of RAD52 and ORC1 selectively impairs the proliferation of cancer cells.

A. Immunoblotting to show levels of FANCD2, RAD52, and ORC1 in the eight cell lines used in this study. Filled triangles indicate a non-specific band detected by the RAD52 antibody. **B**. Cell number (top) and colony forming efficiency (bottom) per siRNA treatment group for HCT116 WT, R52KO (and D2KO) cells. **C**. Cell number per siRNA treatment group for U2OS, RPE1 and BJ cells. **D**. Colony forming efficiency per siRNA treatment group for H1299 and U2OS cells. **E**. Proposed models for mitotic DNA synthesis in cancer (left) and non-cancerous cells (right). In **B-D,** Error bars indicate standard errors of the mean. *, **, and *** indicate $p<0.05$, $p<0.01$ and $p<0.001$ by a t- test, respectively.